Combined Four-Wall Interference Assessment in Two-Dimensional Airfoil Tests

William B. Kemp Jr.*
Virginia Associated Research Campus, Newport News, Virginia
and
Jerry B. Adcock†
NASA Langley Research Center, Hampton, Virginia

Two different procedures are examined for combining the correction method developed by Barnwell and Sewall for the effects of the sidewall boundary layer in two-dimensional wind-tunnel tests with the assessment and correction method due to Kemp for the effects of the upper and lower tunnel walls. One procedure utilizes the similarity transformation defined by Sewall to eliminate velocity perturbations induced by the sidewall boundary layer from consideration in the assessment and correction method as sources of error. The other procedure combines perturbations from all four walls before assessment and correction. In general, the two procedures yield different corrections to Mach number and angle of attack, either of which can be considered valid. Pressure distributions corrected for higher order interference effects are provided by either procedure.

Introduction

In the past decade, several new approaches to the wind-tunnel wall interference problem have been introduced. These new approaches are significant for application to transonic wind tunnels because the wall boundary condition required in the classical methods for predicting wall interference has proven difficult to express accurately for slotted or perforated walls over a range of test conditions. A common feature of the new approaches is their use of data measured on or near the tunnel walls during the test to supplement the data measured on the test model. The adaptive wall approaches[1,2] require two independent sets of data near the walls. The wall-interference assessment and correction approaches[3-11] require static pressure distributions measured on or near the walls to be used either as targets for refining the wall-boundary conditions[3,4] or directly as boundary conditions imposed on flow computations.[5-11] Of the latter procedures, only those of Kemp[9,10] and of Murman[11] utilize transonic computations throughout; the remaining procedures are based either partially or fully on linear superposition of perturbations.

The major development effort to date on all of the procedures mentioned has addressed the two-dimensional application, that is, the testing of airfoil sections in two-dimensional wind tunnels. Efforts are underway, however, to extend both the adaptive wall technology and the assessment and correction technology to three-dimensional tunnel applications. One new development is of concern only to two-dimensional testing and deals with the problem of the boundary layer on the tunnel side walls which act as end plates for the airfoil section under test. Barnwell[12] showed that the flow three dimensionality introduced by perturbations in the displacement thickness of the sidewall boundary layer can be expressed by a two-dimensional governing equation having an appropriate modification to the longitudinal term. He related an equivalent Mach number change to the average displacement thickness on the side walls by use of the Prandtl-Glauert similarity rule. Sewall[13] extended this approach to transonic speeds using the von Kármán transonic similarity rule and showed that results from transonic airfoil tests with artificially thickened sidewall boundary layers could be correlated by the transonic similarity concept.

With the Barnwell-Sewall similarity rule, data measured during a two-dimensional airfoil test with three dimensionality introduced by sidewall boundary layers can be transformed to equivalent data in a true two-dimensional flow at an adjusted Mach number. During development of this procedure, the influence of the tunnel walls above and below the airfoil was ignored. The previously noted wall-interference assessement and correction procedures, on the other hand, were developed to account for the top and bottom wall effects without consideration of the sidewall boundary layer. The present paper addresses the problem of accounting for the effects of both types of interference on a given set of airfoil test data. The method used herein for assessing the top and bottom wall interference is the transonic procedure embodied in the TWINTAN computer program.[14] The experimental data examined are two cases selected from tests of a 12% thick supercritical airfoil in the Langley 0.3-m transonic cryogenic tunnel.[15] One case was entirely subcritical and the other had an extensive supersonic region on the airfoil upper surface terminated by a moderately strong shockwave. The tunnel test section had slotted upper and lower walls and did not utilize boundary-layer removal on the side walls.

Procedures

Sidewall Boundary-Layer Effects

The essential features of the method developed by Barnwell[12] and Sewall[13] for dealing with the sidewall boundary layer are noted here. The first feature is the incorporation of the three-dimensional effects of perturbations in the sidewall boundary-layer displacement thickness into a two-dimensional form of the governing potential equation by replacing the term $(1-M_T^2)$ in the coefficient of the longitudinal potential derivative with $\tilde{\beta}^2$ where

$$\tilde{\beta}^2 = 1 - M_T^2 + 2(\delta^*/b)(2 + 1/H - M_T^2) \quad (1)$$

Presented as Paper 82-0586 at the AIAA 12th Aerodynamic Testing Conference, Williamsburg, Va., March 22-24, 1982; submitted March 3, 1982; revision received Jan. 3, 1983. This paper is declared a work of the U.S. Government and therefore is in the public domain.

*Senior Research Scientist. Associate Fellow AIAA.
†Research Scientist. National Transonic Facility Aerodynamics Branch. Member AIAA.

and b is the tunnel width. The boundary-layer displacement thickness δ^* and shape factor H are taken as constants descriptive of the average or empty tunnel sidewall boundary layer at the model location.

The second feature is the use of (δ^*/b) as a parameter in a family of flows related by transonic similarity rules so that the tunnel flow can be transformed into a similar flow in which $\delta^*=0$. The transformed Mach number M_∞ is that which satisfies

$$M_\infty/(1-M_\infty^2)^{3/4}=M_T/\tilde{\beta}^{3/2} \tag{2}$$

and the pressure and force coefficients are transformed by multiplying the tunnel values by $\tilde{\beta}/\sqrt{1-M_\infty^2}$. For more detail, the reader is directed to Refs. 12, and 13.

Upper and Lower Wall Interference

The wall-interference assessment and correction procedure used in the TWINTAN computer program is illustrated in Fig. 1. The program utilizes three separate solutions of an extended transonic small disturbance equation. The first solution is a numerical reconstruction of the wind-tunnel flow which satisfies boundary conditions that are the measured static-pressure distributions on the test airfoil and at both the upper and lower walls. The airfoil resulting from this solution can be characterized either by its singularity distribution (velocity vector jump across the airfoil) or by its equivalent inviscid shape (ideally, the airfoil plus boundary-layer displacement thickness).

The second solution in TWINTAN computes the model perturbation. This is a free-air solution which uses the singularity distribution as airfoil boundary conditions. During this solution, the far-field Mach number is updated in order to produce a match of the total velocity magnitude at a specified point on the airfoil with that obtained in the tunnel flow solution. This far-field Mach number is the corrected Mach number and the difference between the perturbations of these first two solutions is the perturbation field attributable to the upper and lower walls.

The third solution is another free-air solution at the corrected far-field Mach number, but in this case, the airfoil is represented by its equivalent inviscid shape. The angle-of-attack correction is determined during this solution as that which satisfies the Kutta condition for the value of lift measured in the tunnel. It should be emphasized that this third solution is basically an inverse of the tunnel-flow solution except that the outer boundary condition represents a free-air flow at the corrected Mach number. In the vicinity of the airfoil, care was exercised to make the numerics and boundary conditions consistent with the tunnel-flow solution. The airfoil pressure distribution calculated in this solution, therefore, is simply the original input distribution as modified by the change in outer boundary conditions and far-field Mach number. This calculated distribution is compared with the original measured pressures (now reduced using the corrected Mach number) to give a measure of the residual interference not accounted for by the Mach number and angle-of-attack corrections. The nonuniformity in the wall-induced velocity perturbations over the airfoil is another measure of the residual interference.

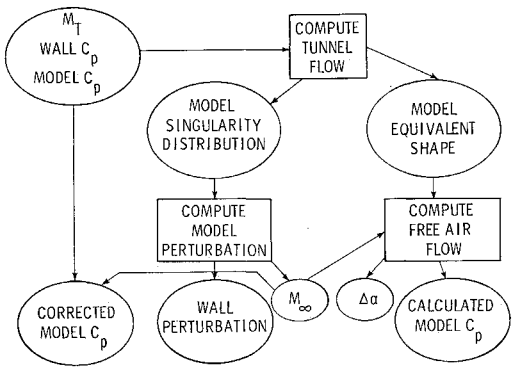

Fig. 1 Flow of data in the TWINTAN program.

Combined Interference

Two procedures have been utilized in the present study for combining the corrections for the sidewall boundary layer and the upper and lower wall interference. One procedure, herein referred to as the unified procedure, allows the TWINTAN program to recognize the combined effects of the sidewall boundary layer and the upper and lower walls as a unified wall-induced perturbation field. This is accomplished simply by altering the governing equation used for the tunnel-flow solution in the TWINTAN program to include the sidewall boundary layer term used by Barnwell and Sewall in the coefficient of the longitudinal derivative. The governing equation used for the two free-air solutions remains unaltered so the TWINTAN procedure will now seek the Mach number and angle of attack of an unconfined two-dimensional flow which produces the same loading distribution as that measured in the confined, quasi-three-dimensional tunnel flow over the same airfoil shape. It is important to note that the unified procedure avoids altogether the concept of flow similarity.

The other, or sequential, procedure is a sequential application of the similarity rule and the unaltered TWINTAN method. Because the TWINTAN program was developed under the assumption that both the wind-tunnel flow and the free-air flow to which it is corrected are strictly two dimensional, it is logical to apply the similarity procedure first to remove the three dimensionality introduced by the sidewall boundary layer and then use the similarity-scaled data in place of wind-tunnel data as inputs to the TWINTAN program.

Results

Strong Shock Case

The test case having a moderately strong shock was obtained at a nominal Mach number (M_T) of 0.7838 with a lift coefficient of 0.601. Based on the surveys made in the empty tunnel, the sidewall displacement thickness parameter $(2\delta^*/b)$ at the model location was found to be 0.0168. Results from the various interference assessment procedures applied to the strong shock case are summarized in Table 1 in the form of corrected Mach number, renormalized lift coefficient and angle-of-attack correction. More detailed results are discussed in the following sections.

TWINTAN Assessment Alone

Figure 2 illustrates results from the TWINTAN analysis of this case with no consideration of the sidewall boundary layer. In this figure, as in some of the subsequent figures, the results are shown in two parts. The first part shows the wall-induced velocity components, Δu and Δv, along the tunnel axis from about one chord upstream to about one chord downstream of the airfoil. The match-point location (i.e, where the local velocity was matched) is shown by the circle symbol on the Δu curve. The value of Δu at this point is the velocity increment corresponding to the Mach number correction. In accordance with past practice for supercritical cases, the match point was specified at the shock location, thereby matching the shock strength in the two flows and minimizing nonuniformities in Δu and Δv near the shock. For this case, however, significant nonuniformities exist through the supercritical region. The angle-of-attack correction is shown by the square symbol plotted at the trailing-edge location and, as is usually the case, approximates an average value of Δv over the rear portion of the airfoil. In the second part of the figure, the experimental pressure distribution, renormalized using the corrected Mach

number, is compared with the pressures calculated in free air over the equivalent inviscid airfoil shape. The discrepancies shown by this comparison are related to the nonuniformities over the airfoil in Δu and Δv.

It should be pointed out that, in the basic TWINTAN program, the renormalization of the experimental pressure coefficients is performed under the assumption that the local pressures and the stagnation pressure were measured accurately in the tunnel. As a result, during renormalization, the experimental pressure coefficients might undergo a significant change in level corresponding to the shift in freestream static pressure, as well as being scaled by an adjusted dynamic pressure. The local Mach number at each orifice, however, remains unchanged as does the level of the critical pressure coefficient C_p^* relative to the experimental points. The calculated free-air pressure distribution, on the other hand, tends to respond to a small change in M_∞ primarily with a shift in shock location, if a shock exists, but with essentially no change in the general level of pressure coefficients.

Table 1 Summary of interference corrections for the strong shock case

Procedure	M_{Int}	M_∞	c_l	$\Delta\alpha$, deg
Original data		0.7838	0.6010	
TWINTAN		0.7913	0.5940	−1.01
Unified		0.7751	0.6094	−1.02
Sequential	0.7688	0.7771	0.6006	−1.02

Unified Procedure

As was previously noted, under the unified procedure, the sidewall boundary layer was accounted for simply by altering the governing equation only for the tunnel-flow computation. The remaining computations including the renormalization of pressure coefficients were unaltered from the basic TWINTAN program. Results from this procedure, with the match point again specified at the shock, are shown in Fig. 3.

The wall-induced velocities show a large discontinuity in Δu and spike in Δv at the shock. Because of the change in the governing equation for the tunnel flow only, it apparently is no longer possible to reproduce the tunnel-flow shock strength in the model perturbation computation by matching the velocity at the shock. As an alternate scheme for selecting the particular value of Δu to be associated with the M_∞ correction, a range of match-point locations was run, the rms difference between the calculated and adjusted experimental C_p distributions was evaluated for each, and the match-point location giving the minimum rms C_p discrepancy was chosen as optimal. This scheme embodies a philosophy akin to that used by Murman[11] who employed a search for the free-air Mach number and angle of attack to minimize a C_p error function.

The ΔC_p optimizing scheme produced the results shown in Fig. 4. The wall-induced velocities are more nearly continuous across the shock, but they now include contributions from both the sidewall boundary layer and the upper and lower wall interference. Consequently, both the Δu nonuniformity and the C_p discrepancy are accentuated over those shown in

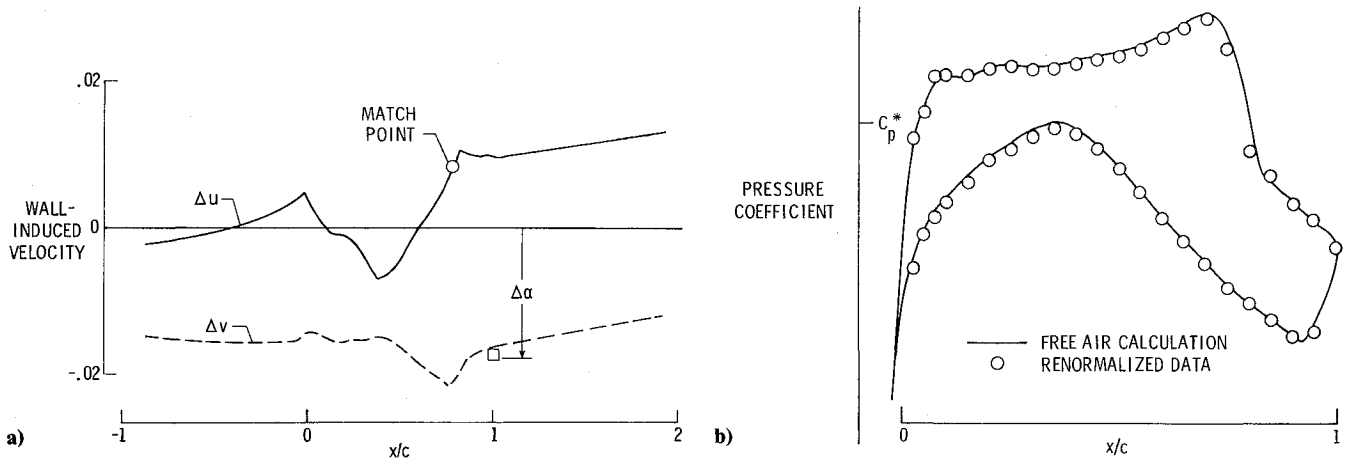

Fig. 2 Results of interference assessment of the strong shock case by the TWINTAN program alone. a) Wall-induced velocities. b) Airfoil pressure distributions.

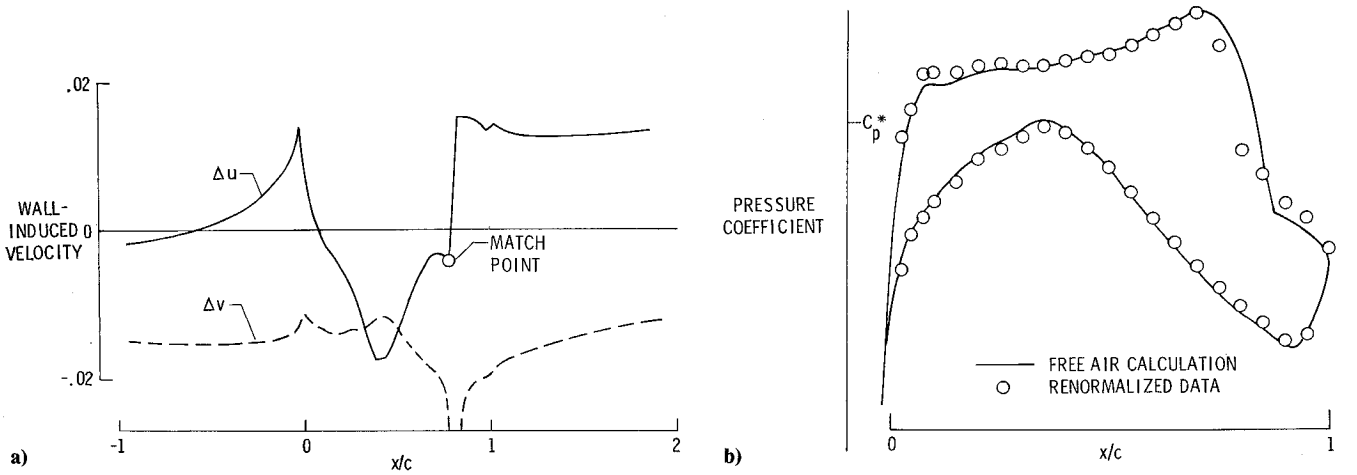

Fig. 3 Results of interference assessment of the strong shock case by the unified procedure, match point located at the shock. a) Wall-induced velocities. b) Airfoil pressure distributions.

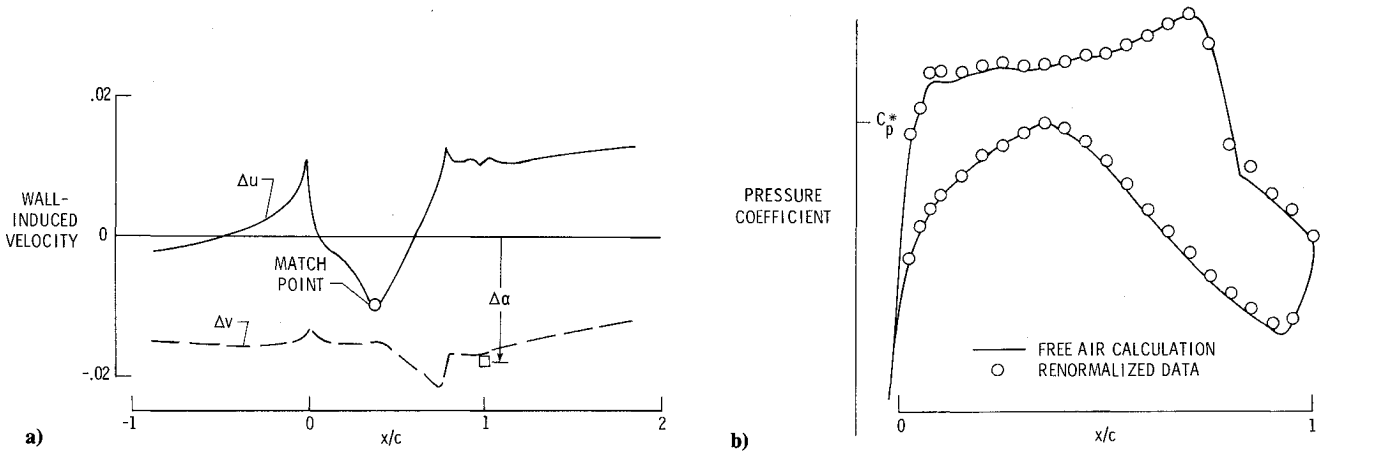

Fig. 4 Results of interference assessment of the strong shock case by the unified procedure, match point located by C_p optimization. a) Wall-induced velocities. b) Airfoil pressure distributions.

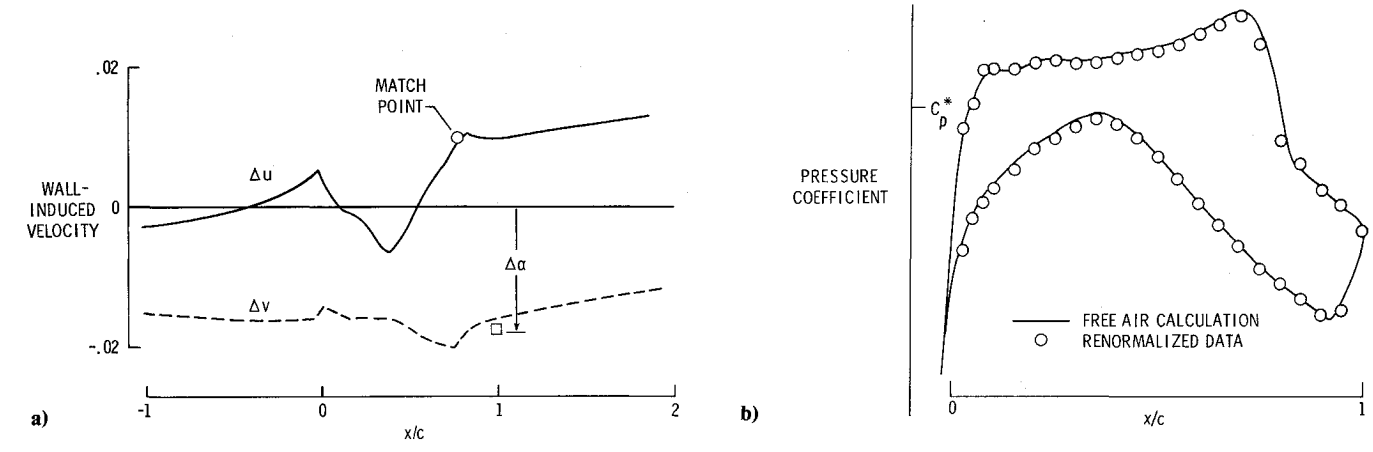

Fig. 5 Results of interference assessment of the strong shock case by the sequential procedure, match point located at the shock. a) Wall-induced velocities. b) Airfoil pressure distributions.

Fig. 2. The corrected Mach number is now below the nominal value instead of above, as was the case in Fig. 2. Apparently, the sidewall boundary layer calls for a negative Mach number correction which more than compensates for the positive correction due to the upper and lower walls. As shown in Table 1 for this strong shock case, the angle-of-attack correction is essentially unaffected by accounting for the sidewall boundary layer regardless of the procedure used.

Sequential Procedure

To apply the sequential procedure, Sewall's similarity rule was applied to find an intermediate (two-dimensional) Mach number of 0.7688 and the corresponding C_p factor of 1.013 was applied to the airfoil and wall C_p values to form the TWINTAN input. The resulting wall-induced velocities, shown in Fig. 5 for the match point at the shock, include only the upper and lower wall effects and appear very similar to those of Fig. 2, as do also the C_p discrepancies.

At this point, a basic philosophical difference between the unified and sequential procedures should be recognized. The flow perturbations due to the varying thickness of the sidewall boundary layer are treated in the unified procedure as part of the total wall-induced perturbation field. A free-air Mach number is sought for which the calculated pressure distribution best matches the measured pressures. Nonuniformities in the wall-induced velocity at the model due to the sidewall boundary layer remain as a high-order component of wall interference. In the sequential procedure, however, the similarity transformation is used to identify a far-field Mach number for which the perturbations due to the sidewall boundary layer and observed at the center of the tunnel become a part of the total perturbation field appropriate to a truly two-dimensional flow. The nonuniformities in the perturbation velocities induced by the sidewall boundary layer are no longer attributable to wall interference in the transformed flow. Consequently, although the wall-induced velocity distributions shown on Fig. 5a were calculated only as the effect of the upper and lower walls, they can be interpreted as the total four-wall interference except that they do not include the constant Δu increment corresponding to the Mach number reduction involved in the similarity transformation.

As indicated in Table 1, the unified procedure achieved C_p optimization by requiring a Mach number reduction which is of the same order as that introduced by the similarity transformation used in the sequential procedure. Because the small difference between the final corrected Mach numbers produces an insignificant change in shock location, the calculated free-air pressure distributions from the two procedures are essentially identical. The renormalized data, however, differ appreciably with the C_p levels from the unified procedure, being significantly more negative than those from the sequential procedure. The difference arises from the fact that, in the unified procedure, the experimental C_p adjustment is made from the nominal Mach number of 0.7838 to the final Mach number of 0.7751 under the assumption of constant stagnation pressure, while the

sequential procedure involves a scaling from 0.7838 to 0.7688 using the transformation factor followed by a constant stagnation pressure adjustment back to 0.7771. It is interesting to note that the discrepancies between the experimental and calculated C_p values can be correlated closely with the departure of the local wall-induced Δu from the level of Δu at the match point. For the unified procedure, the C_p values from the experiment depart in the negative direction from the calculated free-air values in just those regions of the airfoil where the local wall-induced Δu is markedly greater than the match-point level. Similarly, for the sequential procedure, the largest positive departure of the experimental C_p occurs at about 40% chord where the local Δu lies farthest below the Δu at the match point.

Validation Checks

It is recognized that the treatment of the sidewall boundary-layer effects by the method of Barnwell and Sewall is somewhat simplified. It embodies the assumption that the spanwise velocities vary linearly across the tunnel width, and it ignores the boundary-layer interaction with vertical pressure gradients. As a result, the effects of vortices which form at the airfoil-sidewall junctures, and to a lesser extent in the tunnel corners, are ignored, and excessive concentration of sidewall boundary-layer effects probably occurs in high-gradient regions, such as in the vicinity of the airfoil leading edge. The similarity transformation is derived using small-disturbance assumptions and, finally, sidewall boundary-layer separation is ignored. It is of interest, therefore, to search for clues to the realism of the procedures discussed herein.

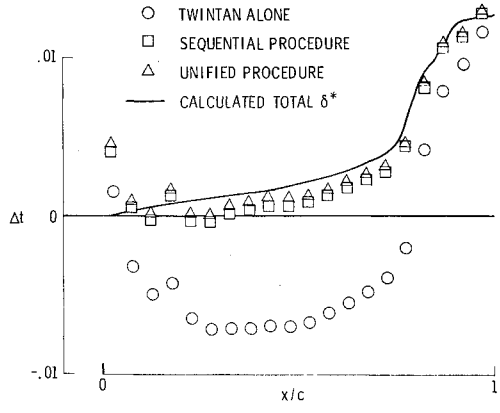

Fig. 6 Effect of accounting for the sidewall boundary layer on the equivalent body thickness distribution.

One such clue is provided by the results shown in Fig. 6. The Δt which is plotted against chordwise location is the excess of the thickness of the equivalent body calculated in the TWINTAN tunnel-flow solution over the actual geometric thickness of the test airfoil. Ideally, Δt should agree with the sum of the displacement thickness of the upper and lower surface boundary layers. The summed displacement thickness from a theoretical boundary-layer calculation is included, therefore, for comparison. The negative values of Δt, obtained without any accounting for the sidewall boundary layer, indicate a significant deficiency in the TWINTAN-alone computation of the wind-tunnel flow. This deficiency is essentially eliminated when the sidewall boundary layer is accounted for by either the similarity rule in the sequential procedure or the altered governing equation in the unified procedure. This result implies that even the simplified treatment of the sidewall boundary layer utilized herein is sufficient to provide an order of magnitude improvement in the realism of the equivalent inviscid airfoil thickness distribution.

To check the similarity rule, a detailed numerical comparison was made between a free-air flow satisfying the altered governing equation and a true two-dimensional flow. The results verified that the difference between the perturbations in the two flows (after accounting for transformation scaling of the potential gradients) essentially vanished when the transformed flow was solved at the far-field Mach number indicated by the similarity rule. The results also verified that the similarity scaling factor for C_p as given by Sewall adequately represented the transformation of pressure coefficients calculated from the velocity perturbations by the exact C_p equation.

As a final check on the interference corrections, the corrected airfoil pressure distributions obtained using the sequential procedure and the unified procedure are compared with theoretically predicted pressure distributions in Figs. 7a and b, respectively. The theoretical results were obtained using the GRUMFOIL program,[16-18] which embodies methods for both the inviscid flow and the boundary-layer calculations which are at the forefront of presently available technology. The airfoil coordinates specified to the program were those actually measured on the test airfoil model, which might explain the waviness apparent in the theoretical curves. The theoretical results were obtained for the test Reynolds number and for the values of M_∞ and c_l given in Table 1 for each interference procedure. The calculated total δ^* curve shown on Fig. 6 was obtained from the same GRUMFOIL run as the theoretical pressure distribution on Fig. 7b.

The renormalized experimental data obtained from the unified procedure are in better agreement with the theoretical

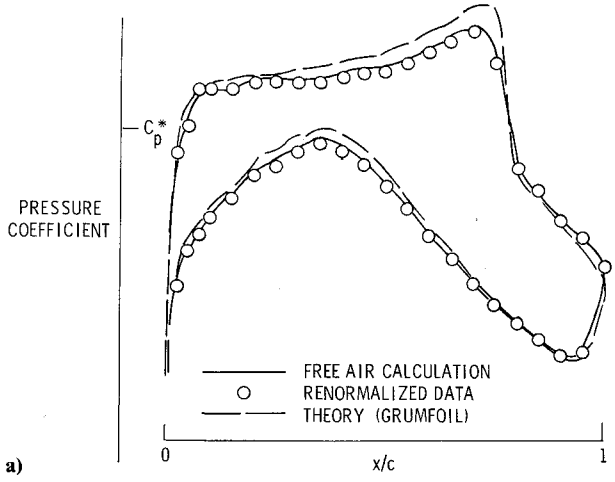

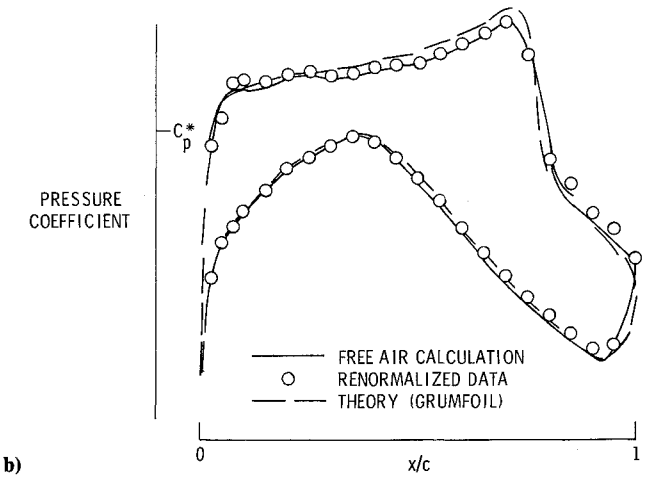

Fig. 7 Comparison with theory of the corrected airfoil pressure distribution for the strong shock case. a) Sequential procedure. b) Unified procedure.

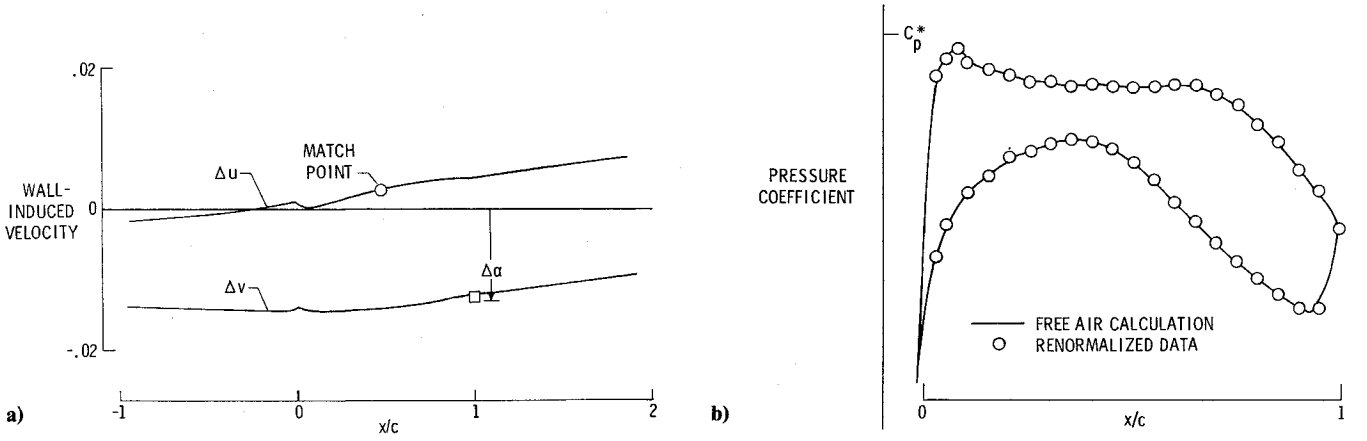

Fig. 8 Results of interference assessment of the subcritical case by the sequential procedure. a) Wall-induced velocities. b) Airfoil pressure distributions.

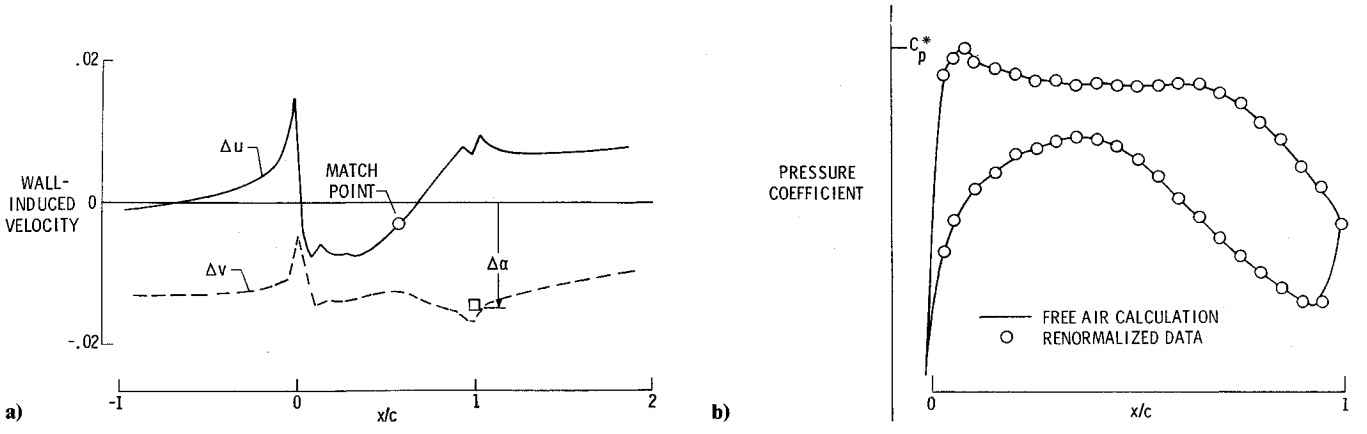

Fig. 9 Results of interference assessment of the subcritical case by the unified procedure. a) Wall-induced velocities. b) Airfoil pressure distributions.

distribution than those from the sequential procedure. Because these data still contain the influence of nonuniformity of wall-induced velocities, it is probably more meaningful to consider the calculated free-air distribution as the more fully corrected result from the wall-interference procedure. On this basis, although the unified procedure might still be judged to give better agreement with theory, its superiority is not impressive and the remaining discrepancies call for some explanation. These discrepancies are not of the type that one would expect from an error in either M_∞ or c_ℓ and the airfoil thickness was well reproduced in the assessment procedures. It is possible that some sidewall boundary-layer separation at the shock could have contributed to the discrepancies. Other causes might be factors not considered in the present study, such as the effects of noise and turbulence in the tunnel or the effects of the isentropic assumption in the inviscid flow theory.

Subcritical Case

A test point having a nominal Mach number (M_T) of 0.6981 and lift coefficient of 0.5193 was selected as a shock-free case. The sidewall boundary displacement thickness parameter ($2\delta^*/b$) was 0.018. Interference corrections from the various procedures are summarized for the subcritical case in Table 2.

Sequential Procedure

The results from use of the sequential procedure are shown in Fig. 8. Although mild gradients are apparent in both components of wall-induced velocity, their distribution along the model chord is relatively free of local irregularities. This is characteristic of TWINTAN results for subcritical cases, and it is appropirate in such cases to locate the match point near midchord so that the blockage correction will approximate an average value of Δu at the airfoil. The resulting agreement between the experimental and calculated free-air pressure distributions is almost exact.

Table 2 Summary of interference corrections for the subcritical case

Procedure	M_{Int}	M_∞	c_l	$\Delta\alpha$, deg
Original data		0.6981	0.5193	
TWINTAN		0.7001	0.5172	−0.73
Unified		0.6960	0.5215	−0.86
Sequential	0.6820	0.6841	0.5252	−0.71

Unified Procedure

The results from the unified procedure are shown in Fig. 9. The wall-induced velocities are now dominated by the nonuniformities introduced by the sidewall boundary-layer perturbation. It is interesting to note that the Δu distribution over the airfoil resembles the shape of the mean airfoil pressure distribution. For this subcritical case, the ΔC_p minimization scheme adopted for locating the match point was free of the shock location constraint and could, therefore, select a Mach number for which the experimental C_p values were renormalized to best approximate the calculated level. The resulting agreement between the experimental and

calculated pressure distributions is still very good in spite of the less uniform wall-induced velocities.

The summary of interference corrections given in Table 2 shows that the corrected Mach number from the unified procedure is significantly higher than that from the sequential procedure. This difference arises directly from the similarity transformation which utilized a Mach number reduction of 0.0161 to eliminate the sidewall boundary-layer effects as an error source. With no shock location constraint, the unified procedure was not forced to the same corrected Mach number. The angle-of-attack corrections given in Table 2 also differ between the two procedures. A comparison of the Δv curves in Figs. 8a and 9a implies that there is some change in wall-induced downwash associated with the sidewall boundary-layer effects which leads to the different values of $\Delta\alpha$. This difference in $\Delta\alpha$ is probably related to the combination of differences in renormalized lift coefficient and corrected Mach number given in Table 2.

Concluding Remarks

Two procedures for combining the interference effects from the two-dimensional tunnel sidewall boundary layer with an assessment and correction procedure for the upper and lower wall interference have been compared. In the unified procedure, the flow perturbations introduced by the sidewall boundary layer are combined with those from the upper and lower walls and the total interference field is assessed to determine corrections. In the sequential procedure, a similarity transformation is utilized to identify a new Mach number at which the flow perturbations due to the sidewall boundary layer become an appropriate part of a true two-dimensional flow and need no longer be considered in the procedure as a source of error. The transformed flow is then assessed for upper and lower wall interference for which further corrections are applied. The thickness distribution of the equivalent airfoil shape resulting from the tunnel flowfield computation within either procedure was found to be much more realistic than that obtained without accounting for the sidewall boundary layer. This result demonstrates the appropriateness of the representation by either procedure of the sidewall boundary-layer effects.

In general, the two procedures yield different corrections to Mach number and angle of attack, either of which can be considered valid. When a strong shock was present, however, the two procedures produced nearly the same corrections to Mach number and angle of attack so that the shock location in the tunnel flow would be duplicated in the flow corrected by either procedure. The calculated free-air pressure distribution was found to be less dependent on the procedure than was that obtained by renormalizing the measured pressures. Because the calculated distribution is also corrected for higher order interference effects, its use as the corrected pressure distribution is recommended.

References

[1] Ferri, A. and Baronti, P., "A Method for Transonic Wind-Tunnel Corrections," *AIAA Journal*, Vol. 11, Jan. 1973, pp. 63-66.

[2] Sears, W. R., "Self-Correcting Wind Tunnels," *The Aeronautical Journal*, Vol. 78, Feb./March 1974, pp. 80-89.

[3] Mokry, M., Peake, D. J., and Bowker, A. J., "Wall Interference on Two-Dimensional Supercritical Airfoils, Using Wall Pressure Measurements to Determine the Porosity Factors for Tunnel Floor and Ceiling," National Research Council of Canada, Aero. Rept. LR-575, Feb. 1974.

[4] Blackwell, J. A., "Wind-Tunnel Blockage Correction for Two-Dimensional Transonic Flow," *Journal of Aircraft*, Vol. 16, April 1979, pp. 256-263.

[5] Mokry, M. and Ohman, L. H., "Application of the Fast Fourier Transform to Two-Dimensional Wind-Tunnel Wall Interference," *Journal of Aircraft*, Vol. 17, June 1980, Vol. 17, pp. 402-408.

[6] Capelier, C., Chevalier, J. P., and Bouniol, F., "Nouvelle Methode de Correction des Effets de Parois en Courant Plan," *La Récherche Aero-Spatiale*, Jan./Feb. 1978, pp. 1-11.

[7] Sawada, H., "A General Correction Method of the Interference in Two-Dimensional Wind Tunnels with Ventilated Walls," *Transactions of the Japan Society for Aeronautical and Space Sciences*, Vol. 21, Aug. 1978, pp. 57-68.

[8] Aulehla, F., "Grenzen der Widerstandbestimmung schlanker Korper in transsonischen Windkanalen," Messerschmitt-Bolkow-Blohm, UFE 13150, June 1976.

[9] Kemp, W. B. Jr., "Toward the Correctable-Interference Transonic Wind Tunnel," *AIAA Ninth Aerodynamic Testing Conference*, June 1976, pp. 31-38.

[10] Kemp, W. B. Jr., "Transonic Assessment of Two-Dimensional Wind-Tunnel Wall Interference Using Measured Wall Pressure," NASA CP-2045, March 1978, pp. 473-486.

[11] Murman, E. M., "A Correction Method for Transonic Wind-Tunnel Wall Interference," AIAA Paper 79-1533, July 1979.

[12] Barnwell, R. W., "Similarity Rule for Sidewall Boundary-Layer Effect in Two-Dimensional Wind Tunnels," *AIAA Journal*, Vol. 18, Sept. 1980, pp. 1149-1151.

[13] Sewall, W. G., "The Effects of the Sidewall Boundary Layers on Two-Dimensional Subsonic and Transonic Wind Tunnels," *AIAA Journal*, Vol. 20, Sept. 1982, pp. 1253-1256.

[14] Kemp, W. B. Jr., "TWINTAN: A Program for Transonic Wall Interference Assessment in Two-Dimensional Wind Tunnels," NASA TM 81819, May 1980.

[15] Ray, E. J., Ladson, C. L., Adcock, J. B., Lawing, P. L., and Hall, R. M., "Review of Design and Operational Characteristics of the 0.3-Meter Transonic Cryogenic Tunnel," NASA TM-80123, 1979.

[16] Melnik, R. E., Chow, R., and Mead, H. R., "Theory of Viscous Transonic Flow Over Airfoils at High Reynolds Number," AIAA Paper 77-680, June 1977.

[17] Melnik, R. E., "Wake Curvature and Trailing-Edge Interaction Effects in Viscous Flow Over Airfoils," Advanced Technology Airfoil Research, Pt. 1, Vol. I, NASA CP-2045, 1979, pp. 255-270.

[18] Melnik, R. E., "Turbulent Interactions on Airfoils at Transonic Speeds—Recent Developments," *Computations of Viscous-Inviscid Interactions*, AGARD CP-291, 1981.